

# Mathematical model of extrusion in FDM 3D printing technology

O.B. Kudryashova<sup>✉</sup>, N.E. Toropkov, M.I. Lerner, A.B. Vorozhtsov

National Research Tomsk State University, 36, Lenin's Avenue, Tomsk, Russia, 634050

✉ [olgakudr@inbox.ru](mailto:olgakudr@inbox.ru)

**Abstract.** We proposed a mathematical model of flow and extrusion in the 3D printing process (FDM technology). The model is based on fluid mechanics and uses conservation laws taking into account friction losses and local resistance losses. We performed a parametric study of the model. We have obtained experimental data on the rheology of compositions based on bimodal powders containing micro- and nanoparticles. The rheological properties of low-filled mixtures of powders with polymer differ from those of highly-filled mixtures of bimodal powders. These data are used as the basis for calculating the extrusion rate of compositions in FDM 3D printing of the considered compositions. The results of calculations of the extrusion rate depending on temperature, pressure, and dispersion of powders are given in the report. The search for optimal printing parameters based on mathematical modeling of the process is the goal of this work.

**Keywords:** extrusion, 3D printing, FDM technology, bimodal powders, mathematical mo

**Acknowledgement.** *The study was supported by a grant from the Russian Science Foundation (project No. 21-79-30006).*

**Citation:** Kudryashova OB, Toropkov NE, Lerner MI, Vorozhtsov AB. Mathematical model of extrusion in FDM 3D printing technology. *Materials Physics and Mechanics*. 2022;50(3): 388-400. DOI: 10.18149/MPM.5032022\_3.

## 1. Introduction

The technology of layer-by-layer deposition (Fused deposition modeling, FDM) is most often used in additive technologies for creating three-dimensional objects [1]. This method is based on the application of fused fiber material to the platform, which makes it possible to design and implement new materials, including composites. Usually, a polymer thread is used as a material for creating objects, but recently there have been attempts to apply this technology for printing polymeric materials modified with various powders (steel, aluminum, wood ash, termites, etc.) [2-5].

Commonly used additive technologies for working with metal powders are SLS (Selective Laser Sintering) and SLM (Selective Laser Melting) [5]. They involve the use of expensive and complex equipment, including a powerful laser. FDM 3D printing technology is based on the use of a relatively simple and inexpensive printer. This is the most used 3D printing technology due to the relative simplicity and availability of devices, as well as the ability to adjust operating parameters over a fairly wide range of values.

Typically, a polymer thread is used for this printer. If a polymer composition with metal powders is used instead of a thread, then the problem of using the FDM technology lies in the high viscosity of the material, which is especially high at a high concentration of particles.

The classic version of FDM technology uses thermoplastic polymers or composites based on them, which are heated in the hot part (hotend) of the print head to a molten or semi-liquid state, and then flow through the extruder die onto the platform or over previously printed layers. The thermoplasticity of the polymer thread is an essential property of this method. It allows the filaments to melt and solidify at room temperature after printing [6]. Usually, a composite filament for printing is prepared in advance, but in some cases, a mixture of filler and polymer powders is fed directly into the print head of the printer, where these powders are mixed and melted [7].

The complexity of using FDM, as well as some other additive technologies, is associated with the high viscosity of the material, which often depends non-linearly on operating parameters. To overcome the problem of high viscosity ( $> 1000$  Pa s) and reduce friction in the printing process, for example, ultrasound inside the nozzle is used [8]. Bimodal metal powder, which exhibits high fluidity even at a high volume content in the mixture, could be a promising raw material for extrusion additive manufacturing [9].

The choice of operating parameters of the FDM printing process for working with viscous highly filled materials is an urgent task. Very few works are devoted to the theoretical study of this process. Meanwhile, mathematical modeling will reveal the main patterns of the process and the dependence of the target characteristics of printing on operating parameters.

Several theoretical works are devoted to the issues of mathematical modeling of various additive processes: Selective laser melting (SLM) [10-12]; Direct Metal Deposition (DMD) [13], and Direct ink writing (DIW) [14,15]. Meanwhile, few theoretical studies are devoted to FDM technology. The authors of [16] optimize the parameters of the FDM process using hybrid statistical methods. They take into account a number of competing process parameters, including layer thickness, build orientation, fill density, and number of loops. Recent work [7] investigated the effect of HMX solids content and particle size on the viscosity of molten TNT/HMX explosives. The authors used computational fluid dynamics methods to simulate the influence of viscosity, pressure, temperature, nozzle diameter, and particles on fluid flow inside a 3D printer nozzle.

Fluid mechanics methods allow us to identify the most significant characteristics that affect the target parameters of the printing process. However, there are no systematic works describing the features of the technology and the ongoing processes using the selected methods.

Extrusion speed is one of the most important parameters that must be controlled during the printing process. Too low or too high speed leads to deformation of the target object, associated with excessive or insufficient cooling, or poor adhesion of the layers. You can choose the optimal speed using the printer settings when printing with known polymer filament. But it will be difficult to set up printing with more viscous composite formulations without knowing the patterns of viscosity and extrusion rate changes depending on the main control parameters. The control parameters include the feed pressure of the mixture, the heating temperature, the fineness of the powder, and its concentration in the mixture.

The purpose of this work is to determine the extrusion rate of a viscous liquid containing particles and the influence of control parameters on the speed of FDM printing based on mathematical modeling and the application of fluid mechanics methods.

## **2. Mathematical model of the flow of a viscous liquid in a nozzle**

Let us consider a mixture of polymer powder and particles that is fed into a nozzle using a piston/screw. In the heating block (hot end) of the nozzle, the mixture is heated to a predetermined temperature. The viscosity of the resulting liquid depends significantly on temperature and pressure.

From the point of view of reducing the viscosity of the material, it is better to use a lower concentration of particles [17]. Therefore, the concentration of particles is one of the most important parameters that must be optimized. As the experiment shows, the dispersion of particles also significantly affects the viscosity of the material [9].

**Formulation of the problem.** A mixture of polymer and powdered particles of a given volume concentration  $\varphi$  is placed in the nozzle heating block (Hot end). The mixture is heated to a given temperature  $T$ , greater than or equal to the melting point of the polymer; the mixture is acted upon by a piston with a given pressure  $P_p$ . Further, the viscous mixture flows inside the nozzle and outflows from it at a certain velocity  $V_e$ . It is necessary to determine this speed depending on the control parameters ( $T$ ,  $P_p$ ,  $\varphi$ ), as well as the critical values of the parameters at which extrusion is impossible. The geometry of the nozzle is shown schematically in Fig. 1.

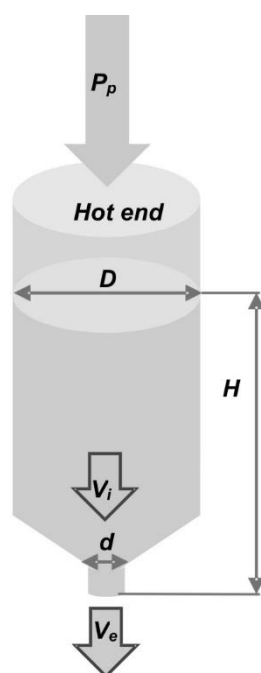


**Fig. 1.** Nozzle scheme

In accordance with the continuity equation the outflow velocity  $V_e = V_i \frac{D^2}{d^2}$ , where  $V_i$  is the velocity of the liquid inside the nozzle,  $D$  is the diameter of the wide part,  $d$  – is the diameter of the nozzle,  $H$  is the height of the extruder.

Bernoulli's equation for a viscous fluid:

$$\frac{\Delta P}{\rho g} + \frac{V_i^2}{2g} = -H + \frac{V_e^2}{2g} + h_g + h_{loc} = -H + \frac{V_i^2 D^2}{2g d^2} + h_g + h_{loc}, \quad (1)$$

where  $\Delta P = P_p - P_{atm}$  is the extrusion pressure (relative to atmospheric),  $h_g$  is hydraulic friction losses, with the laminar flow:  $h_g = \frac{64 H V_i^2}{Re D 2g}$  (Darcy-Weisbach formula),  $Re = \frac{\rho D V_i}{\eta}$ ,  $\eta$  is the dynamic viscosity of the medium.

There is no flow at the inlet, and the velocity is equal to zero, at the bottom near the nozzle outlet is  $V_i$ . According to the conditions of the problem, friction losses due to viscosity are significant.

The nozzle is characterized by losses due to local resistance (sudden narrowing of the flow). Hydraulic losses due to local resistance are expressed by the Altshul formula [18]:

$$h_{loc} = \left( \frac{1-\varepsilon}{\varepsilon} \right)^2, \quad \varepsilon = 0.57 + \frac{0.043}{1.1 - D^2/D^2}. \quad (2)$$

Since the Re number includes the  $V_i$ , we have a quadratic equation for the velocity inside the tube. It is a positive decision:

$$V_i = \frac{-b + \sqrt{b^2 - 4ac}}{2a}, \quad \text{где } a = \frac{1 - D^2/d^2}{2g}, \quad b = -\frac{32\eta}{gD^2}, \quad c = H - h_{loc} + \frac{\Delta P}{\rho g}. \quad (3)$$

The first speed limit is the absence of a solution to the quadratic equation (3). It occurs when the following condition is met:

$$b^2 = 4ac, \quad \text{or} \quad \left( \frac{32\eta}{gD^2} \right)^2 = 4 \left( H - h_{loc} + \frac{\Delta P}{\rho g} \right) \left( \frac{1 - D^2/d^2}{2g} \right). \quad (4)$$

In this case, the rate is:

$$V_i = \frac{-b}{2a} = \frac{32\eta(1 - D^2/d^2)}{D^2}. \quad (5)$$

**Simplifications.** Consider the Bernoulli equation in the dimensionless form:

$$\frac{\Delta P}{\rho g H} = -1 + \frac{V_i^2}{2gH} \left( \frac{D^2}{d^2} - 1 \right) + \frac{h_g}{H} + \frac{h_{loc}}{H}. \quad (6)$$

Let us estimate the value of different terms of the equation. Let us find the conditions under which one or another term can be neglected.

At high viscosity, the term of the equation responsible for the kinetic energy of the liquid can be neglected. Then the equation will take the form:

$$\frac{\Delta P}{\rho g H} = -1 + \frac{h_g}{H} + \frac{h_{loc}}{H}. \quad (7)$$

This is done if:

$$\frac{V_i^2}{2g} \left( \frac{D^2}{d^2} - 1 \right) \ll h_g, \quad \text{или} \quad \text{Re} \ll \frac{64}{((D/d)^2 - 1)} \frac{H}{D}. \quad (8)$$

From here we get a simplified expression for the rate inside the structure:

$$\frac{\Delta P}{\rho g H} = -1 + \frac{32V_i \eta}{g\rho D^2} + \frac{h_{loc}}{H}. \quad (9)$$

From here we get a simplified expression for the rate inside the structure:

$$V_i = \left( 1 + \frac{\Delta P}{\rho g H} - \frac{h_{loc}}{H} \right) \cdot \frac{g\rho D^2}{32\eta}. \quad (10)$$

With a relatively high-pressure drop, i.e. at  $\frac{\Delta P}{\rho g H} \gg 1 - \frac{h_{loc}}{H}$ , the expression for the velocity can be further simplified:

$$V_i \approx \frac{\Delta P D^2}{32\eta H}. \quad (11)$$

Taking into account the continuity equation, we obtain an expression for the outflow

$$\text{velocity: } V_e \approx \frac{\Delta P}{32\eta H} \frac{D^4}{d^2} = A_1 \frac{\Delta P}{\eta}, \quad (12)$$

where  $A_1 = \frac{D^4}{32Hd^2}$  – constant characterizing the geometry of the nozzle.

Expression (12), which is correct under conditions of high fluid viscosity and sufficiently high piston pressure, makes it possible to obtain explicit dependences of the extrusion rate on the control parameters – pressure and viscosity. Viscosity, in turn, depends on temperature, pressure, and particle concentration.

**Accounting for the dependence of viscosity on temperature, pressure and particle concentration.** The dependence of the viscosity of thermoplastics on temperature is determined by the Frenkel-Eyring equation [19]:

$$\eta = \eta_{0T} \cdot \exp\left(-\frac{E_a}{RT}\right), \quad (13)$$

where  $\eta_{0T}$  is a constant having the dimension of viscosity,  $E_a$  is flow activation energy,  $R$  is the universal gas constant;  $R = 8.32 \text{ J}/(\text{mol}\cdot\text{K})$ ;  $T$  is thermodynamic temperature, K.

The dependence of viscosity on pressure is also exponential:

$$\eta = \eta_{0P} \cdot \exp(\beta\Delta P), \quad (14)$$

where  $\beta$  is exponential pressure coefficient,  $\eta_{0P}$  is a constant having the dimension of viscosity.

Combining (13) and (14) we obtain the expression:

$$\eta = \eta_0 \cdot \exp\left(-\frac{E_a}{RT}\right) \cdot \exp(\beta\Delta P). \quad (15)$$

At low-pressure drops ( $\Delta P$  less than 800 MPa) and temperature ( $\Delta T$  less than 200 K), a linear approximation of the dependence of viscosity on these parameters can be used [20]:

$$\eta = \eta_0 \cdot (1 + \alpha_T \Delta T + \beta_P \Delta P). \quad (16)$$

In [21], the rheological properties of mixtures of poly(vinylidene fluoride) (PVDF) and polyethylene (LDPE) in the molten state were studied. Values of flow activation energy for different shear rates ( $\tau = 3\text{-}10 \text{ s}^{-1}$ ) are obtained, which are 41.95-55.37 kJ/mol for PVDF. The corresponding PVDF melt viscosities at 190°C are 4 to 7.5 kPa·s.

According to the conditions of the problem, we have not just a polymer melt, but a melt containing particles. Einstein established the dependence of the viscosity of a solution on the concentration of suspended particles [22]:

$$\eta = \eta_0 (1 + \alpha\varphi), \quad (17)$$

where  $\varphi$  is volume fraction of the dispersed phase;  $\alpha$  is coefficient depending on the particle shape. For spherical particles  $\alpha = 2.5$ ; for elongated particles  $\alpha > 2.5$ . This equation was derived under the assumption that the particles of the dispersed phase are much larger than the matrix molecules, they are distant from each other, have the same size and shape, and do not interact.

Subsequent experiments showed [23] that formula (17) is valid only for  $\varphi \leq 10^{-3}$ . Einstein's theory was generalized to the case of higher volume concentrations. As a result, for the effective viscosity coefficient, a relation of the form was obtained:

$$\eta = \eta_0 (1 + \alpha\varphi + k\varphi^2), \quad (18)$$

where the coefficient  $k \sim 6\text{-}6.25$ .

**Influence of control parameters on blend viscosity and extrusion rate (Parametric Model Study).** Below are the calculated dependences of the viscosity and extrusion rate on the control parameters in accordance with the proposed mathematical model.

The rate depends inversely on viscosity (Fig. 2). The calculation is made for  $D = 3 \text{ mm}$ ,  $H = 0.1 \text{ m}$ ,  $D^2 / d^2 = 36$  ( $A_1 = 0.1 \text{ mm}$ ).

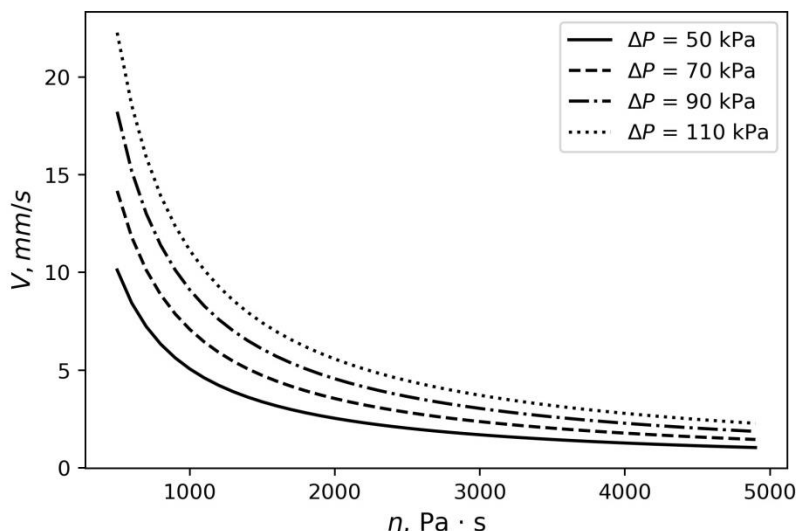


**Fig. 2.** Extrusion Rate vs. Viscosity

We obtained the dependence of the extrusion rate on temperature taking into account the exponential dependence of viscosity on temperature (13) and the data of work [21] (Fig. 3). The calculation is made for  $E_a = 60$  kJ/mol,  $\eta_{0T} = 10E+10$  Pa·s,  $A_1 = 0.1$  mm.

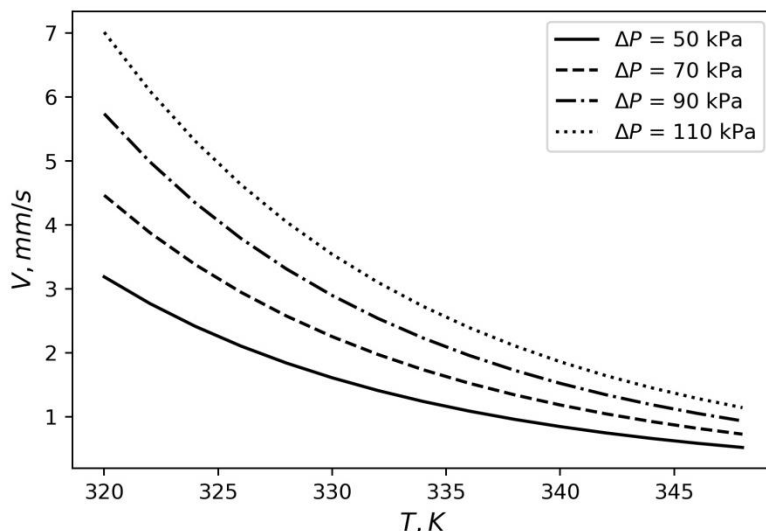


**Fig. 3.** Temperature dependence of extrusion rate

We calculated the dependence of the extrusion rate on pressure, taking into account the exponential dependence of viscosity on pressure (14) for given parameters  $E_a = 60$  kJ/mol,  $\eta_{0P} = 10E+10$  Pa·s,  $A_1 = 0.1$  mm,  $\beta = 0.05$  (Fig. 4).

The obtained dependencies correspond in character to those obtained in [7] using nozzle simulation in FDM technology.

The extrusion rate decreases with increasing temperature and pressure, which is not intuitively obvious. However, with increasing pressure, the velocity can not only decrease (Fig. 5, calculation at  $\beta = 0.005$ ).

As follows from expression (12), the dependence on the geometric factor  $A_1$  is linear (Fig. 6).

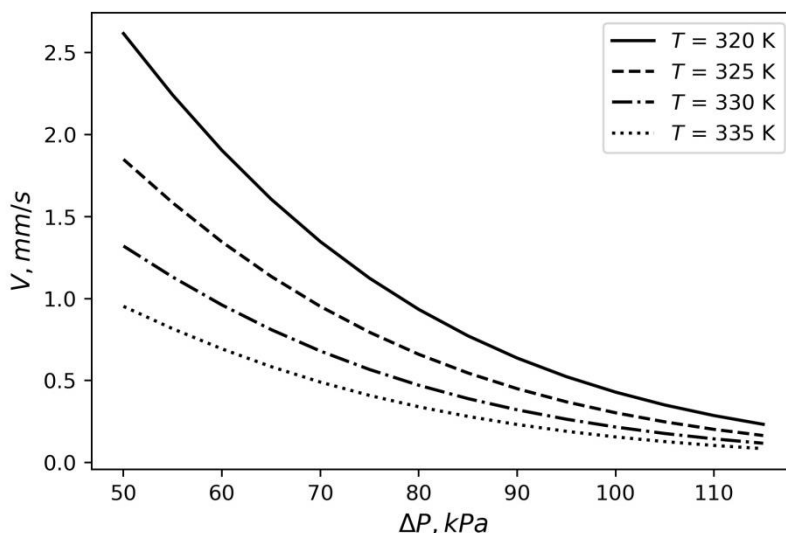


**Fig. 4.** Extrusion rate versus pressure ( $\beta = 0.05$ )

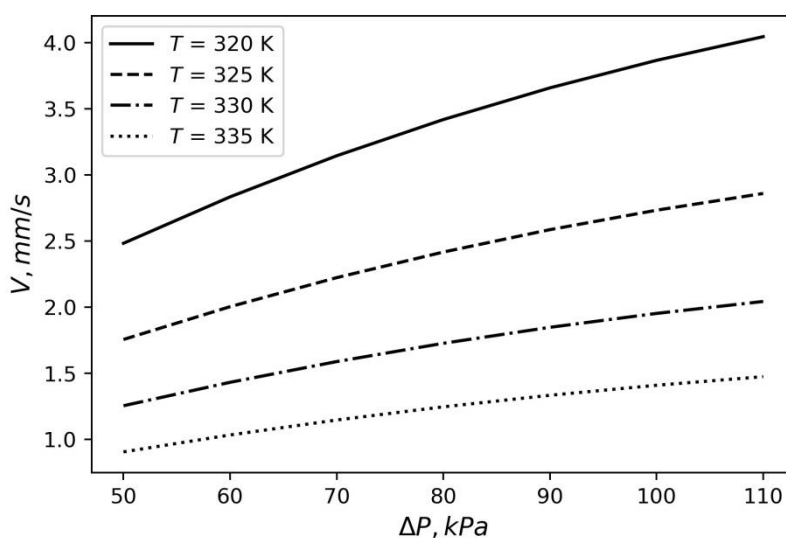


**Fig. 5.** Extrusion rate versus pressure ( $\beta = 0.005$ )

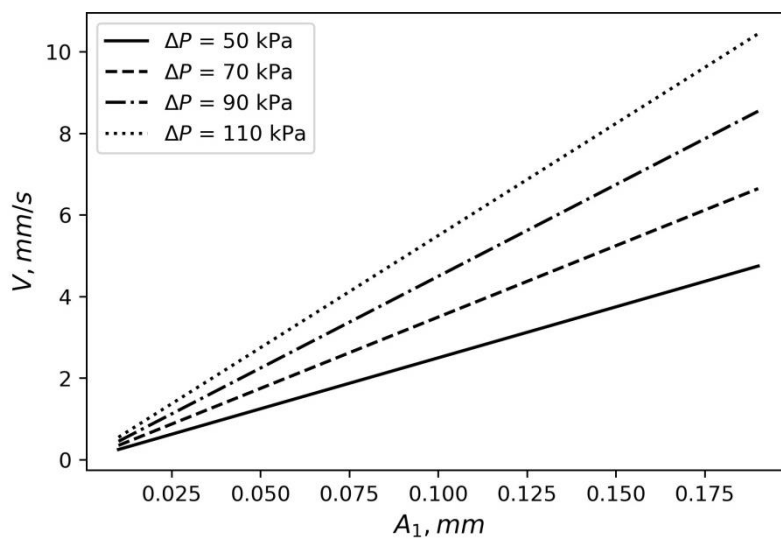


**Fig. 6.** Dependence of the extrusion rate on the geometric factor

The dependence on the concentration of particles in the mixture, calculated by equation (18), is shown in Fig. 7.

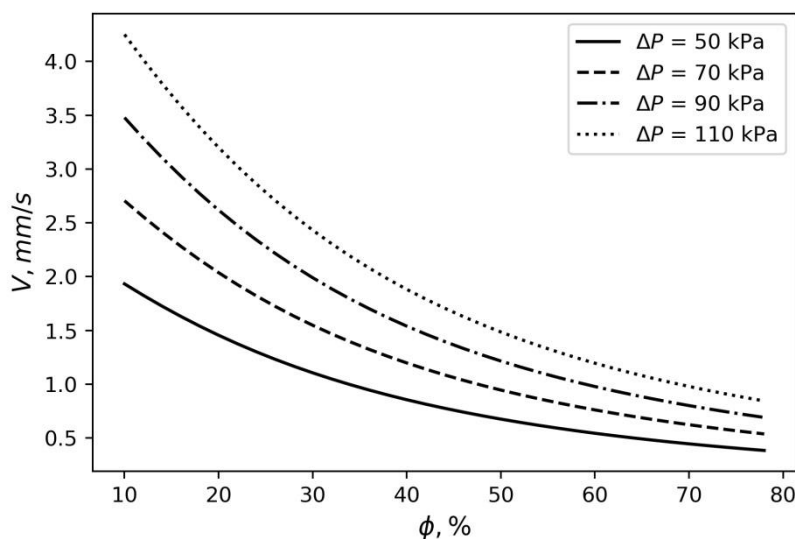


**Fig. 7.** The dependence of the extrusion rate on the concentration of solid particles in the mixture

The results obtained are intuitive: the smaller the proportion of particles in the polymer, the lower the viscosity of the mixture, and the higher the extrusion rate.

As can be seen, the lower the temperature of the mixture, the lower the viscosity and the higher the extrusion rate. Thus, operating the nozzle at the lowest temperature sufficient to melt the polymer is preferred.

### 3. Experiment

**Materials and methods.** A mixture of powders of micro- and nanoparticles was obtained by the method of the electrical explosion of wires (EEW) with a controlled ratio of dispersed phases in one technological process [9, 24]. Bimodal powders obtained by EEW do not require additional mixing and do not separate into fractions, like mixtures of micro- and nanopowders.

The dispersion of the obtained powders was measured using a laser diffraction particle size analyzer MASTERSIZER 2000 (Malvern Panalytical, UK).

The melt flow index (MFI) for all composites was measured with the plastometer IIRT-M (LOIP, Russia) with a load of 1-50 kg at 130-160°C. The measurement of MFI was carried out according to ISO 1133. The MFI index is related to the dynamic viscosity  $\eta$  [25]:

$$\eta = \frac{A \cdot \rho \cdot L}{\text{MFI}}, \quad (18)$$

where the constant  $A = 155.709 \text{ kg} \cdot \text{m}/\text{s}^2$ ,  $\rho$  is material density [ $\text{g}/\text{cm}^3$ ],  $L$  is the load [kg], MFI is the melt flow index [ $\text{g}/10 \text{ min}$ ]. The load application area is  $S_p = 69.3626 \text{ mm}^2$ , thus, pressure is  $P = L/S_p$ .

The binder is a ready-made mixture of polymer marked Viscowax 331 (Innospec, Germany) with the addition of 0.5% stearic acid. The binder content is 63% vol.

**Rheological characteristics of bimodal powder (experimental results). Extrusion rate depending on pressure and temperature (calculation).** To study the rheological characteristics, a bimodal powder of 316L stainless steel was taken, obtained at various energies of an electric explosion (32, 60, 93 J/mm<sup>2</sup>, further indicated by the corresponding



numbers) with different dispersity, as well as a powder with a characteristic particle size of the order of tens of micrometers (designated "micron") (Table 1).

Table 1. Median values of powder dispersion

Sample	10% $D$ ( $\mu\text{m}$ )	50% $D$ ( $\mu\text{m}$ )	90% $D$ ( $\mu\text{m}$ )
32	0.157	1.777	3.421
60	0.123	1.209	2.561
93	0.102	1.112	2.145
Micron	10.965	17.357	29.777

Figure 8 shows the experimental dependence of viscosity on temperature, and Fig. 9 shows the experimental dependence of viscosity on pressure for these powders.

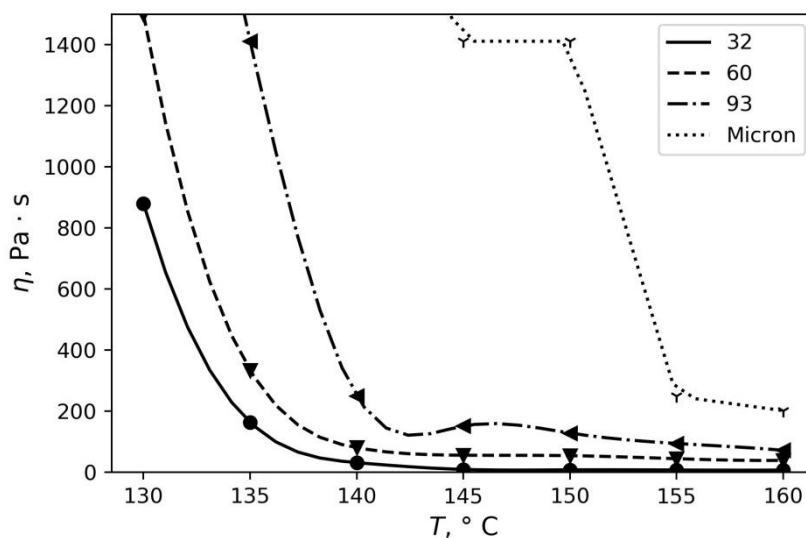


Fig. 8. Temperature dependence of viscosity obtained experimentally for four powders of different dispersion

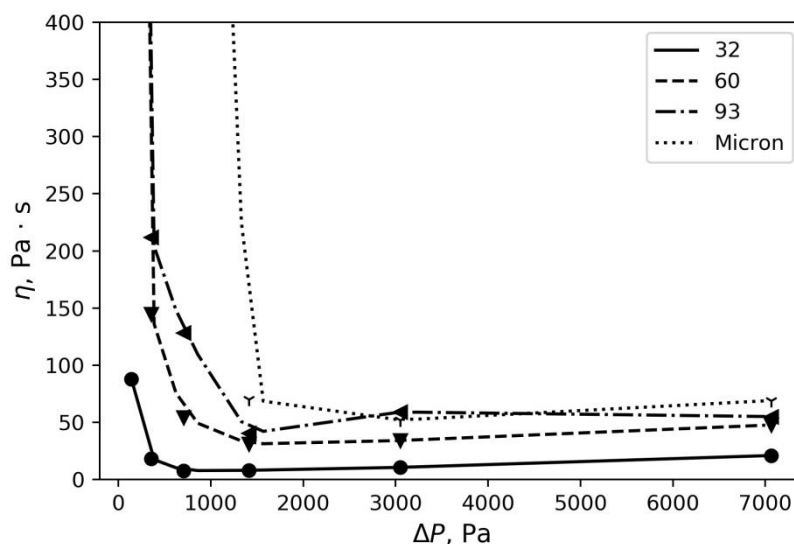
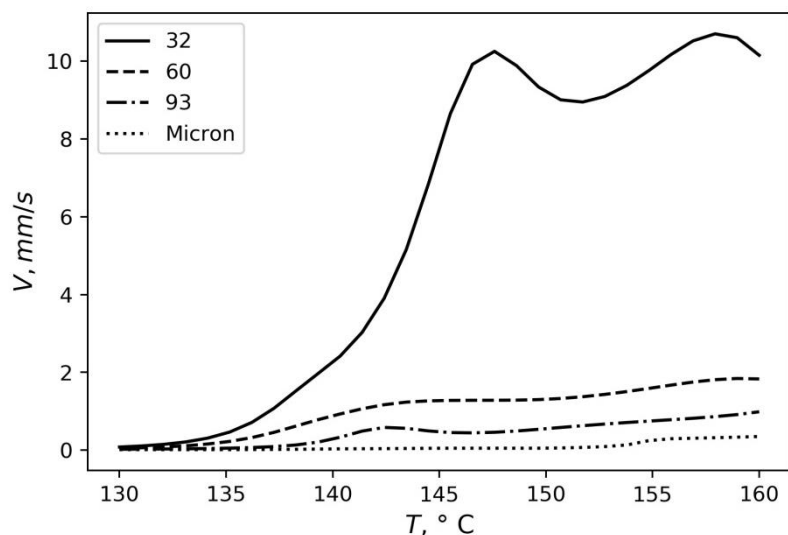


Fig. 9. Pressure dependence of viscosity obtained experimentally for four powders of different dispersion

The flow of the mixture, as follows from the obtained data, has a pronounced threshold character: at a pressure below a certain value, the viscosity is very high, then at a pressure of

about 1-1.5 MPa, the viscosity becomes minimal. Then it gradually grows linearly. At temperatures below  $\sim 140-145^{\circ}\text{C}$ , the viscosity is also very high, then it drops sharply, and then decreases with temperature in accordance with a linear law.

The lowest viscosity in the experiment was obtained for the powder obtained at explosion energy of  $32.5 \text{ J/mm}^2$ , which has a relatively large fraction of micron-sized particles. On the other hand, a powder with only micron-sized particles, without nanoparticles, has the highest viscosity. Substituting the experimental dependences of viscosity on temperature and pressure into formula (12), we obtain the dependence of the extrusion rate on temperature (Fig. 10) and pressure (Fig. 11).



**Fig. 10.** Dependence of the extrusion rate on temperature, taking into account the experimental dependence of viscosity on temperature for four powders of different dispersion

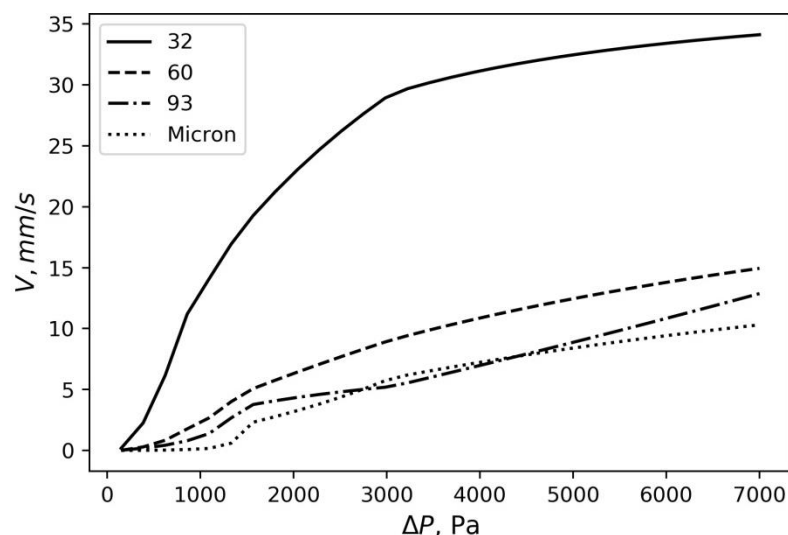


**Fig. 11.** Dependence of the extrusion rate on pressure, taking into account the experimental dependence of viscosity on pressure for four powders of different dispersion

The extrusion rate grows weakly with temperature and pressure for all powders, except for powder "32" with the most pronounced bimodality. Nanoparticles in a bimodal powder play the role of liquid molecules, with micron-sized particles suspended there. Such a pseudo-liquid, as shown by the experiment, has a lower viscosity than highly filled thermoplastic mixtures with particles of the same size.

#### 4. Conclusion

The paper proposes a mathematical model of the 3D printing process (FDM technology) of materials based on polymer binders and powders. The model is based on the integral equations of continuum mechanics. Reasonable simplifications adequate to the case under consideration are carried out. A simple relation (12) is obtained, which relates the extrusion rate to the control parameters of the system: pressure, geometrical characteristics of the nozzle, and mixture viscosity. The dependences of the viscosity of the mixture on pressure, temperature, and the content of the dispersed phase are considered. A parametric study of the model was carried out. The obtained dependences correspond to the data of other researchers for similar materials and FDM technology.

The rheological properties of low-filled mixtures of powders with polymer differ from those of highly-filled mixtures of bimodal powders. The paper presents experimental data on the rheological properties of mixtures containing bimodal powders, depending on pressure, temperature, and dispersion composition. A threshold dependence was found: at pressure and temperature below a certain value (1-1.5 MPa, 140-145°C), the viscosity is very high, which makes it impossible or difficult to flow. After this threshold, the viscosity decreases slightly with temperature and slightly increases with pressure. Estimates of the extrusion rate of this starting material were carried out, based on the proposed model and the experimental results obtained.

#### References

1. Camargo JC, Machado ÁR, Almeida EC, Silva EF MS. Mechanical properties of PLA-graphene filament for FDM 3D printing. *The International Journal of Advanced Manufacturing Technology*. 2019;103(5): 2423-2443.
2. Dudek P. FDM 3D printing technology in manufacturing composite elements. *Archives of metallurgy and materials*. 2013;58(4): 1415-1418.
3. Ramazani H, Kami A. Metal FDM, a new extrusion-based additive manufacturing technology for manufacturing of metallic parts: a review. *Progress in Additive Manufacturing*. 2022;7: 609–626.
4. Gonzalez-Gutierrez J, Godec D, Guráň R, Spoerk M, Kukla C, Holzer C. 3D printing conditions determination for feedstock used in fused filament fabrication (FFF) of 17-4PH stainless steel parts. *Metallurgija*. 2018;57(1-2): 117-120.
5. Mazurchevici AD, Nedelcu D, Popa R. Additive manufacturing of composite materials by FDM technology: A review. *Indian Journal of Engineering and Materials Sciences (IJEMS)*. 2021;27(2): 179-192.
6. Ngo TD, Kashani A, Imbalzano G, Nguyen KT, Hui D. Additive manufacturing (3D printing): A review of materials, methods, applications and challenges. *Composites Part B: Engineering*. 2018;143: 172-196.
7. Zong H, Cong Q, Zhang T, Hao Y, Xiao L, Hao G et al. Simulation of Printer Nozzle for 3D Printing TNT/HMX Based Melt-Cast Explosive. *The International Journal of Advanced Manufacturing Technology*. 2022;119: 3105-3117.
8. Gunduz IE, McClain MS, Cattani P, Chiu GC, Rhoads JF, Son SF. 3D printing of extremely viscous materials using ultrasonic vibrations. *Additive manufacturing*. 2018;22: 98-103.
9. Pervikov A, Toropkov N, Kazantsev S, Bakina OV, Glazkova E, Lerner M. Preparation of Nano/Micro Bimodal Aluminum Powder by Electrical Explosion of Wires. *Materials*. 2021;14(21): 6602.
10. Ökten K, Biyikoğlu A. Development of thermal model for the determination of SLM process parameters. *Optics & Laser Technology*. 2021;137: 106825.

11. Ansari MJ, Nguyen DS, Park HS Investigation of SLM process in terms of temperature distribution and melting pool size: modeling and experimental approaches. *Materials*. 2019;12(8): 1272.
12. Estrada-Díaz JA, Elías-Zúñiga A, Martínez-Romero O, Olvera-Trejo D. Enhanced Mathematical Model for Producing Highly Dense Metallic Components through Selective Laser Melting. *Materials*. 2021;14(6): 1571.
13. Choi J, Han L, Hua Y. Modeling and Experiments of Laser Cladding With Droplet Injection. *ASME. J. Heat Transfer*. 2005;127(9): 978-986.
14. Zhang B, Nguyen AK, Narayan RJ, Huang J Direct ink writing of vancomycin loaded polycaprolactone/polyethylene oxide/hydroxyapatite 3D scaffolds. *Journal of the American Ceramic Society*. 2021;105(3): 1821-1840.
15. Buj-Corral I, Domínguez-Fernández A, Gómez-Gejo A. Effect of printing parameters on dimensional error and surface roughness obtained in direct ink writing (DIW) processes. *Materials*. 2020;13(9): 2157.
16. Deswal S, Narang R, Chhabra D. Modeling and parametric optimization of FDM 3D printing process using hybrid techniques for enhancing dimensional preciseness. *International Journal on Interactive Design and Manufacturing (IJIDeM)*. 2019;13(3): 1197-1214.
17. Knott MC, Craig AW, Shankar R, Morgan SE, Iacono ST, Mates JE, McCollum JM. Balancing processing ease with combustion performance in aluminum/PVDF energetic filaments. *Journal of Materials Research*. 2021;36(1): 203-210.
18. Altshul AD. *Hydraulic resistances*. Moscow: Nedra; 1970.
19. Frenke YI. *Kinetic Theory of Liquids*. M-L.: Akad. Nauk SSSR; 1945. (In Russian)
20. Kerber ML et al. *Technology of polymer processing. Physical and chemical processes*. Moscow: URITE; 2018. (In Russian)
21. Kaseem M, Hamad K, Yang HW, Lee YH, Deri F, Ko YG. Melt rheology of poly(vinylidene fluoride)(PVDF)/low density polyethylene (LDPE) blends. *Polymer Science Series A*. 2015;57(2): 233-238.
22. Sherman P. *Rheology of emulsions*. Oxford: Pergamon Press; 1963.
23. Rudyak VY. *Statistical aerohydrodynamics of homogeneous and heterogeneous media*. Novosibirsk: NSUACE (Sibstrin); 2005. (In Russian)
24. Krinitcyn M, Toropkov N, Pervikov A, Glazkova E, Lerner M. Characterization of nano/micro bimodal 316L SS powder obtained by electrical explosion of wire for feedstock application in powder injection molding. *Powder Technology*. 2021;394: 225-233.
25. Shenoy AV, Saini DR, Nadkarni VM. Melt rheology of polymer blends from melt flow index. *International Journal of Polymeric Materials*. 1984;10(3): 213-235.

## THE AUTHORS

### **Kudryashova O.B.**

e-mail: olgakudr@inbox.ru

ORCID: 0000-0002-0404-8736

### **Toropkov N.E.**

e-mail: zerogooff@gmail.com

ORCID: 000-0003-3146-3043

### **Lerner M.I.**

e-mail: lerner@ispms.tsc.ru

ORCID: 0000-0001-8565-1344

**Vorozhtsov A.B.**

e-mail: [abv@mail.tomsknet.ru](mailto:abv@mail.tomsknet.ru)

ORCID: [0000-0003-2080-9942](https://orcid.org/0000-0003-2080-9942)